Korean J. Chem. Eng., **28**(1), 106-113 (2011)
DOI: 10.1007/s11814-010-0283-7

NH_3 selective catalytic reduction (SCR) of nitrogen oxides (NO_x) over activated sewage sludge char

Yong Beom Jo*, Jin Sun Cha, Jeong Huy Ko*, Min Chul Shin***, Sung Hoon Park****, Jong-Ki Jeon*****, Seung-Soo Kim******, and Young-Kwon Park*,**,†**

*Graduate School of Energy and Environmental System Engineering, University of Seoul, Seoul 130-743, Korea
**School of Environmental Engineering, University of Seoul, Seoul 130-743, Korea
***Material Testing Center, Korea Testing Laboratory, Seoul 152-718, Korea
****Department of Environmental Engineering, Sunchon National University, Suncheon 540-742, Korea
*****Department of Chemical Engineering, Kongju National University, Cheonan 330-717, Korea
******Department of Chemical Engineering, Kangwon National University, Samcheok 245-711, Korea
(*Received 13 May 2010 • accepted 7 June 2010*)

Abstract−The de-NO_x performance of sewage sludge chars activated physically using water vapor or chemically using KOH was evaluated. Characteristics of chars activated under different activation temperatures, water vapor concentrations, and KOH/char ratios were analyzed by N_2 adsorption-desorption and FT-IR. Chemically activated chars were more efficient in removing NO_x due to their higher surface area, oxygen functional group and NH_3 adsorption than physically activated chars. The de-NO_x performance of the activated chars is influenced more by chemical properties such as oxygen functional groups and NH_3 adsorption sites than by physical properties like specific surface area and pore volume.

Key words: Sewage Sludge Char, De-NO_x, Physical Activation, Chemical Activation

INTRODUCTION

Removal of harmful nitrogen oxides (NO_x) from the exhaust presents a great challenge to the catalysis community [1,2]. A variety of investigations have been undertaken to reduce nitrogen oxide (NO_x) emissions, with selective catalytic reduction (SCR) being the most widely used worldwide. A number of studies on catalysts for SCR processes have been carried out [3-6]. The catalysts used most frequently to reduce NO_x emissions from stationary sources (incinerators, power plants) are V_2O_5/TiO_2 (anatase) catalysts mixed with WO_3 or MoO_3. The V_2O_5 catalysts exert high efficiency between 300 and 400 °C. To meet this temperature range, SCR equipment can be installed before particle removal facility and desulfurization equipment. In this case, however, SO_2 and particle matters may cause catalyst deactivation and poisoning. Furthermore, after the particle removal facility and desulfurization equipment whose temperature range is about 250 °C, the effluent gas must be reheated. This reheating creates an extra operational cost. To reduce operational costs, SCR equipment can be installed between the particle removal facility and desulfurization equipment. However, in such a layout, effluent gas also contains SO_2 and As which may cause catalyst deactivation. Accordingly, extensive efforts have been made to develop low-temperature SCR catalysts capable of activation under 250 °C [7-9].

Investigations of SCR using carbon have recently been carried out. Various researchers showed that active carbons exhibit a high catalytic activity for NO reduction with NH_3 at temperature below 300 °C [10]. It is possible to create oxygen functional groups through simple treatment on the surface of carbon material for SCR, which assists the chemical adsorption/degradation of NO_x and hence enhances NO_x removal efficiency at low temperatures [11]. Jüntgen [12] reported data about active coke and activated carbons used as catalysts for the removal of NO_x with ammonia and observed that the catalytic activity influenced functional groups on the carbon surface. Some investigations show that the catalytic activity of carbon materials for NO conversion increases with the oxygen concentration on the carbon surface [13]. Such carbon materials are manufactured in various forms, including activated carbon, carbon fiber, carbon nanotubes, and carbon black. With the exception of activated carbon, however, recently developed carbon materials are too expensive for use in SCR processes. Recently, efforts have been made to produce carbon catalysts using industrial byproducts as well as agricultural byproducts [14-18].

In this study, carbon catalysts were produced using sewage sludge char obtained as a residue from bio-energy generation processes using sewage sludge. The char was activated physically with water vapor or chemically with KOH. The structural characteristics and NO_x removal efficiencies were then evaluated.

EXPERIMENTAL

1. Preparation of Activated Char

Sewage sludge was obtained from J Sewage Treatment Plant in Seoul, Korea, where municipal wastewater is treated using the standard activated sludge method. The sludge, with a water content of approximately 80%, was dried using a disk drier to lower the water content below 10%. To characterize the samples, proximate (mois-

†To whom correspondence should be addressed.
E-mail: catalica@uos.ac.kr

Table 1. Nomenclature of activated chars

	Initial	a	b
SCW-a-b	Physically activated char	Moisture concentration	Activation
SCK-a-b	Chemically activated char	KOH/Char ratio	temperature

ture, volatile matter, ash, fixed carbon), ultimate (C, H, O, N, S), and metal-component analyses were performed for each sample.

To produce the char, pretreated sewage sludge was pyrolyzed in a reactor for 2 h at 600 °C under an N_2 flow of 50 mL/min. For physical activation, the char produced in the previous step was put in a reactor in which the water vapor concentration was controlled between 10 and 80%. The reactor temperature was increased by 5 °C/min from room temperature to an activation temperature designated between 300 and 800 °C, and then maintained for 1 h. 1 N KOH solution was used for chemical activation. The KOH and char were mixed at different weight ratios, such as 0.5 : 1, 1 : 1 and 2 : 1, for 2 h on a hot plate to evaporate the water, and dried for more than 24 h in a 110 °C oven. Then, the dried sample was treated with nitrogen gas in the same way as with the physical activation. To remove the remaining K^+, the samples were washed with 5.0 M HCl and then with distilled water. The washed samples were dried prior to the characterization processes.

2. Characterization

2-1. N_2 Adsorption-desorption

The N_2 adsorption-desorption method was used to measure specific surface area, pore volume, and pore size distribution of the prepared chars as functions of activation conditions. Prior to measurement, the chars were pretreated under a 200 °C vacuum atmosphere (BELSORP-MINI, BEL Japan, Inc.). Specific surface area, total pore volume, and average pore size were determined from the obtained N_2 adsorption-desorption isotherms using the Brunauer-Emmett-Teller (BET) method. The Barrett-Joyner-Halenda (BJH) method was used to determine pore size distribution.

2-2. FT-IR

All FT-IR (Thermo Nicolet 380) analyses were performed from 4,000 to 400 cm^{-1}, with a resolution of 4 cm^{-1}, to identify the oxygen functional groups (-COOH, -OH, -COO, C=O) formed on the char surface using KBr pellets.

2-3. NH_3-TPD

The NH_3 adsorption-desorption characteristics of the chars produced from different activation conditions were examined using the NH_3-temperature-programmed desorption (TPD) method with a TPD/TPR 2900 analyzer (Micromeritics Instrument Co.). Prior to measurement, the samples were first treated in a He stream at 250 °C and then cooled to 100 °C. The NH_3 adsorption was then carried out at 100 °C. After the samples were purged in a He stream for 2 h to remove physically adsorbed NH_3, the chars were heated to 400 °C at a heating rate of 10 °C/min with a 50-mL/min N_2 flow. Desorbed NH_3 was detected with a thermal conductivity detector (TCD).

3. Catalytic De-NO_x Activity

An SUS tubular fixed-bed reactor, with an inner diameter of 130 mm and a height of 1,500 mm, was fabricated to measure the NO_x removal efficiency of the produced chars. The schematic and explanation of the experimental apparatus used in this study can be found in our previous report [5]. The composition of the inlet gas was maintained at 1,000 ppm of NO, 1,000 ppm of NH_3, and 5 vol% of O_2. The W/F (char sample weight/feed flow) ratio was 5.0 g min/L (SV ≒ 6,000 h^{-1}). The NO concentrations of inlet and outlet streams were measured by a NO_x analyzer (42C, Thermo Ins.). After 1 hr reaction time, the NO_x removal efficiency was calculated by the following equation:

$$NO_x \text{ removal efficiency } (\%) = 100 \times \left(\frac{C_{NO}^{i} - C_{NO}}{C_{NO}} \right)$$

C_{NO}^{i}: inlet NO concentration (ppm)
C_{NO}: outlet NO concentration (ppm)

RESULTS AND DISCUSSION

1. Characterization of Activated Chars

Nomenclature of the activated chars used in this study is summarized in Table 1.

Table 2 shows the results of proximate, ultimate, and metal component analyses. The sewage sludge used in this study had a low volatile matter content (46.17% on average) and high ash content (38.57%) compared to other biomass materials, due likely to the soil component being swept in from the grit chamber of the sewage treatment plant and inorganic species abundant in the sewage. The moisture content was 5.23% on average. Also, high contents of C and O might imply that oxygen functional groups (-COOH, -OH, -COO, and C=O) could be created from the char activation. Metal component analysis showed that the concentrations of metal com-

Table 2. Results of proximate, ultimate, and metal component analyses of dried sludge

Proximate (wt%)	Moisture	5.23
	Volatile matter	46.17
	Fixed carbon	10.03
	Ash	38.57
Ultimate (wt%)	C	39.74
	H	6.09
	O	47.49
	N	5.44
	S	1.24
Metal component (mg/kg)	Si	56.1
	Fe	3,780
	Ca	25,030
	Al	26,855
	P	17,405
	K	3,857
	Ti	83.88
	Zn	1,546
	Mg	6,630
	Na	859.7

ponents (Fe, Ca, Al, K, Ti, Zn, Mg) in the sludge were high due to their abundance in the sewage. High content of metal components in the sludge may be favorable for NO_x removal considering that use of select metal components (Fe, Ca) as impregnating agents of carbon catalysts for NO_x reduction has been investigated [19].

1-1. Physically Activated Chars

To investigate the effects of activation temperature on the characteristics of the physically activated char, referred to as SCW hereafter, the char was activated physically at temperatures between 300 and 800 °C and under an N_2 flow of 50 mL/min with a water vapor content of 50%. Table 3 compares specific surface areas and pore characteristics of SCWs activated at different temperatures (SCW-50-from 300 to 800). Both the specific surface area and the total pore volume increased with activation temperature.

Table 3. Characteristics of sludge chars activated by various treatments

Sample	Specific surface area (m^2/g)	Total pore volume (cm^3/g)	Ave. pore diameter (nm)
Sludge char (SC-F-600-2)	49.8	0.043	3.643
SCW-50-300	52.4	0.048	3.548
SCW-50-400	52.9	0.050	3.629
SCW-50-500	55.0	0.057	3.674
SCW-50-600	75.8	0.065	3.706
SCW-50-700	70.8	0.063	3.490
SCW-50-800	79.5	0.078	3.512
SCW-10-700	56.2	0.057	4.032
SCW-20-700	64.1	0.061	3.825
SCW-40-700	68.0	0.060	3.752
SCW-60-700	78.5	0.066	3.375
SCW-80-700	75.9	0.068	3.590
SCK-1.0-500	220.1	0.185	3.359
SCK-1.0-600	471.3	0.303	2.569
SCK-1.0-700	618.7	0.382	2.501
SCK-1.0-800	789.6	0.483	2.449
SCK-0.5-700	434.0	0.346	4.290
SCK-2.0-700	968.1	0.614	2.328

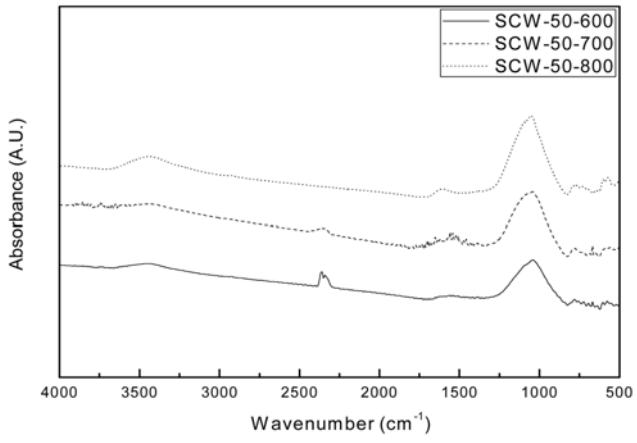

Fig. 1. FT-IR spectra of SCWs activated at different temperatures.

Fig. 1 shows the FT-IR spectra measured to identify the functional groups developed on the surface of SCWs activated at different temperatures. The C-O stretching vibration peak intensity appearing at 1,200-1,100 cm^{-1} was shown to increase with temperature. The intensities of the C=O stretching peak at 1,600 cm^{-1} and the hydroxyl O-H stretching peak at 3,500 cm^{-1} were also shown to increase with temperature [20]. The alkynes CC vibration peak [21] at 2,332 cm^{-1}, however, did not appear at 800 °C. In a study characterizing carbon catalysts prepared from pistachio-nut shells by physical activation, Yang et al. [22] argued that magnitudes of FT-IR band are much higher for carbon activated at a higher temperature because the aromatization reaction, conversion of aliphatic or alicyclic compounds into aromatics, takes place at high temperatures.

To investigate the effect of the water content of the N_2 gas on the characteristics of SCW, the char was activated physically at 700 °C under an N_2 flow of 50 mL/min with water vapor content between 10 and 80%. Table 3 compares the characteristics of the SCWs activated with different water vapor contents (SCW-from 10 to 80-700). The specific surface area increased as the water content increased from 10 to 60 vol%. When the water content increased further to 80 vol%, however, the specific surface area decreased. Similar results have been reported in the literature. Tennant et al. [23] reported in their paper on steam-pyrolysis activation, using wood char, that the specific surface area increased from 605 to 696 m^2/g as the water/carbon weight ratio increased from 0 to 0.085, whereas the specific surface area decreased to 672 m^2/g when the water/carbon weight ratio increased further to 0.170. At these conditions, an important generation of hydrogen may be occurring, whose inhibitory effect in the activation process has been widely reported in literature [24, 25]. This inhibitory effect is thought to be due to the displacement of the equilibrium in the activation reactions or even to a reversible reaction of the hydrogen in the active centers of the carbon matrix that could lead to their deactivation [26].

Fig. 2 shows the FT-IR spectra measured for the SCW activated with different water vapor content. The C-O stretching vibration peak, the C=O stretching peak, and the hydroxyl O-H stretching peaks at 1,200-1,100, 1,600, and 3,500 cm^{-1}, respectively, were all

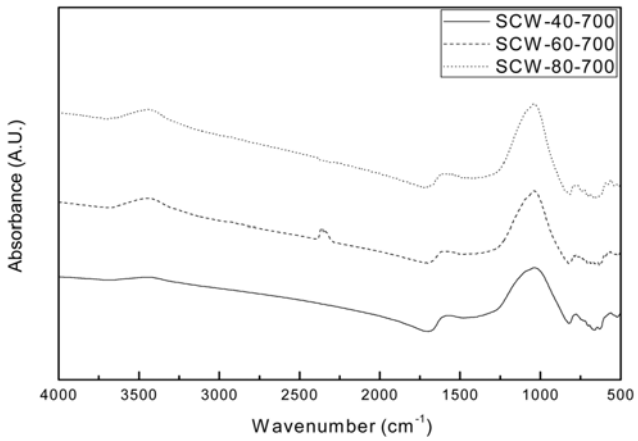

Fig. 2. FT-IR spectra of SCWs activated at different steam concentrations.

shown to increase with water vapor content, indicating that the oxygen functional groups developed more easily on the char surface under a higher water vapor atmosphere. Bouchelta et al. [27] reported that the specific surface area and micropore volume of date stone char increased to 635 m^2/g and 0.716 cm^3/g, respectively, by activation using water vapor. Pistachio-nut shell char also showed increases in specific surface area (821 m^2/g) and pore volume (0.68 cm^3/g) when activated by water vapor [28]. In the present study, however, the maximum specific surface area was 79.5 m^2/g, small compared to the values reported in the literature [27,28]. This is because the ash content, which inhibits pore generation during physical activation, is high in sewage sludge [29].

1-2. Chemically Activated Chars

To investigate the effect of activation temperature on the characteristics of chemically activated char, referred to as SCK hereafter, the char was activated chemically at different temperatures under an N_2 flow of 50 mL/min. The reactor temperature was increased by 5 °C/min from room temperature to an activation temperature, controlled between 500 and 800 °C, and then maintained for 1 h.

Fig. 3 shows the N_2 adsorption-desorption isotherms of SCKs activated at different temperatures. It can be seen that nitrogen adsorption and desorption increased over the entire pressure range, including low pressure conditions ($p/p_0 \fallingdotseq 0$) when the activation temperature increased from 500 to 800 °C. This can be attributed to generation of more micropores and mesopores at a higher temperature as is shown in Fig. 4.

Table 3 compares the characteristics of SCKs activated at different temperatures (SCK-1.0-from 500 to 800). Both the specific surface area and the total pore volume increased with activation temperature: from 220.1 m^2/g and 0.1848 cm^3/g for SCK-1.0-500 to 789.6 m^2/g; 0.483 cm^3/g for SCK-1.0-800.

Fig. 5 shows the FT-IR spectra measured for SCKs activated at different temperatures. Contrary to the results for SCWs, the peak intensities decreased with increasing temperature. Ahmed et al. [30] and Lua et al. [31] attributed this to breakage of chemical bonds in the oxygen functional groups, such as carboxylic group bonds at 700 °C, leading to loss of functional groups *via* evaporation.

To investigate the effects of the KOH/char ratio on the characteristics of SCK, the char was activated at different KOH/char ratios (0.5, 1, and 2). Table 3 compares the characteristics of the SCKs activated with different KOH/char ratios (SCK-from 0.5 to 2.0-700). Fig. 6 shows the N_2 adsorption-desorption isotherms of SCKs activated at different KOH/char ratios. The nitrogen adsorption and

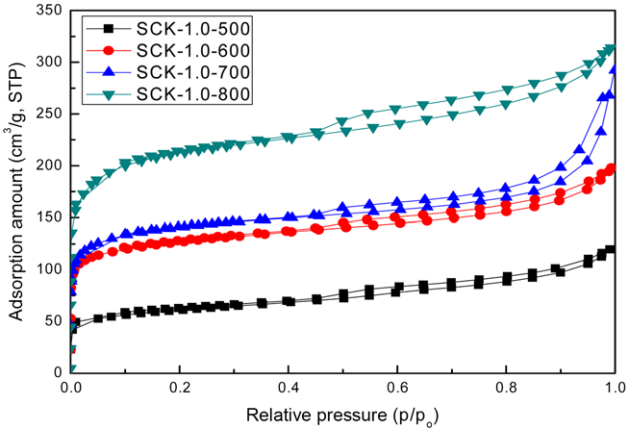

Fig. 3. Nitrogen adsorption/desorption isotherms of SCK at different activation temperatures.

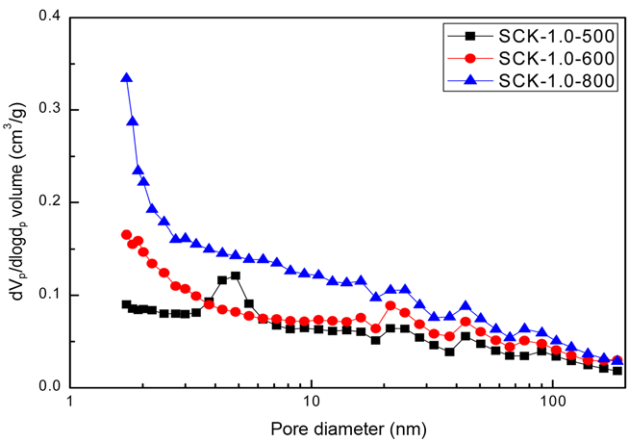

Fig. 4. Effect of activation temperature on pore diameter of SCK.

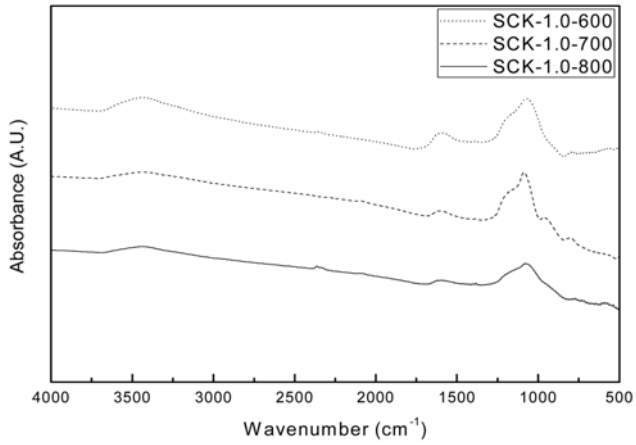

Fig. 5. FT-IR spectra of SCKs activated at different activation temperatures.

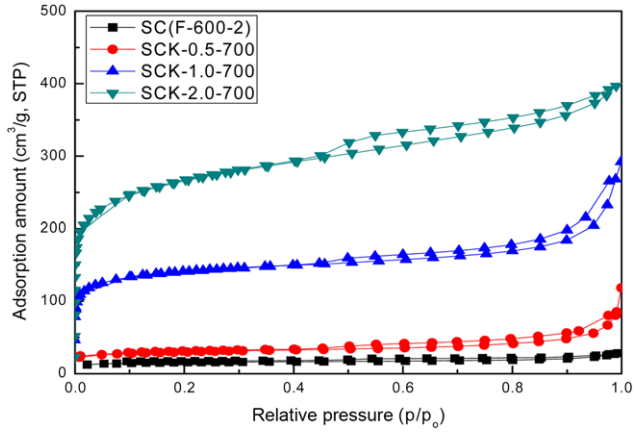

Fig. 6. Nitrogen adsorption/desorption isotherms of sludge chars activated chemically (SCKs) with different KOH ratios.

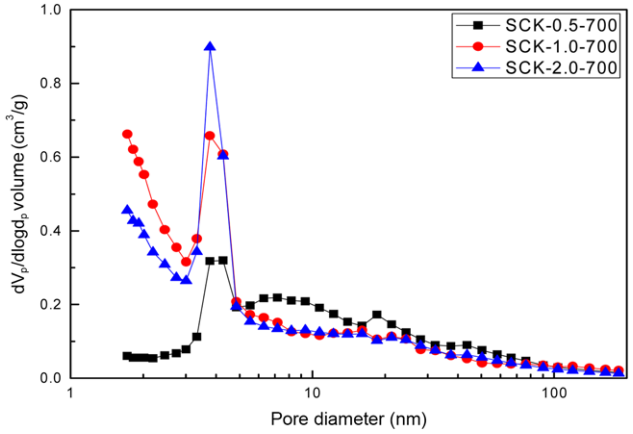

Fig. 7. Effect of KOH/char ratio on pore size distribution of chemically activated sludge chars (SCKs).

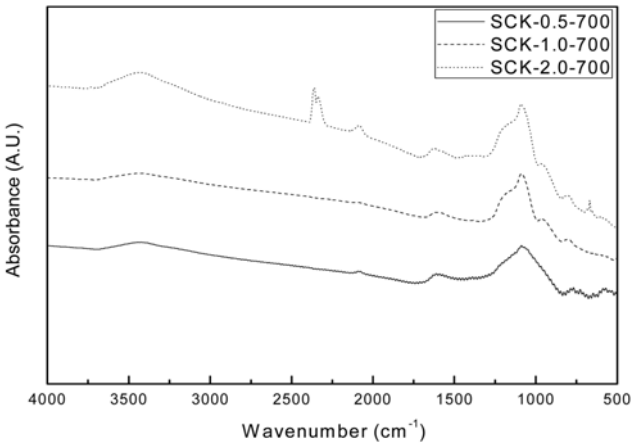

Fig. 8. FT-IR spectra of SCKs activated with different KOH/char ratios.

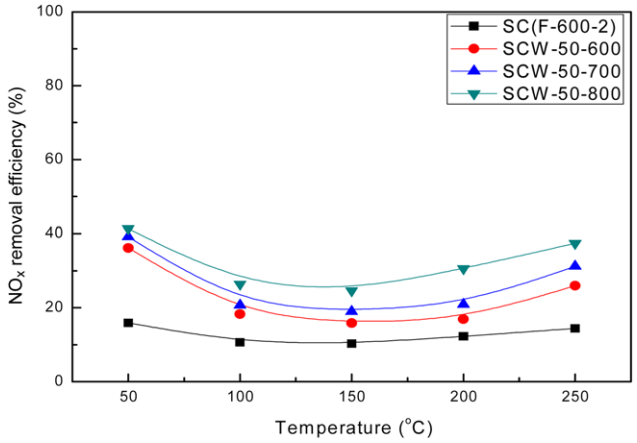

Fig. 9. Effect of activation temperature on NO_x removal efficiency of SCWs at different de-NO_x process temperatures.

Table 4. NH_3-TPD data of sludge chars activated by various treatments

Catalysts	NH_3 desorption (mmol/g)
SCW-50-600	0.011
SCW-50-700	0.013
SCW-50-800	0.016
SCW-40-700	0.009
SCW-60-700	0.014
SCW-80-700	0.015
SCK-1.0-600	0.051
SCK-1.0-700	0.035
SCK-1.0-800	0.028
SCK-0.5-700	0.029
SCK-1.0-700	0.035
SCK-2.0-700	0.070

desorption increased with the KOH/char ratio. Compared with SCW, the adsorption at low pressure ($p/p_0 \fallingdotseq 0$) increased considerably. The average pore size decreased with increasing KOH/char ratio as shown in Table 3. Fig. 7 indicates that it is due to development of micropores at high KOH dosages; K_2CO_3 generated by the activation process reacts with HCl during acid treatment and is then eluted, leaving micropores [32].

$$6KOH+2C \leftrightarrow 2K+3H_2+2K_2CO_3$$

In this study, the specific surface area and pore volume of the activated char were shown to increase with activation temperature and KOH/char ratio. Several studies have reported that the activation agent/carbon ratio is the most important factor for improving char performance through chemical activation [30,33,34]. Fig. 8 shows the FT-IR analysis results of SCKs activated at different KOH/char ratios. Similar to the results for the SCWs, the amount of oxygen functional groups developed on the char surface increased with activation agent content.

2. Catalytic De-NO_x Activity

2-1. SCWs

The NO_x removal efficiencies of SCWs activated at different temperatures are shown in Fig. 9 as a function of the de-NO_x process temperature. Throughout the temperature range tested (50-250 °C), the de-NO_x performance increased as the activation temperature increased from 600 °C to 800 °C. The de-NO_x performance of SCW-50-700 was shown to be better than that of SCW-50-600, although the specific surface area and total pore volume of SCW-50-700 were measured to be smaller than those of SCW-50-600 (Table 3). Analysis for surface functional groups at different activation temperatures (Fig. 1) showed that more oxygen functional groups developed on SCW-50-700 than on SCW-50-600. The NH_3-TPD analysis results (Table 4) showed that NH_3 desorption was also higher for SCW-50-700 than SCW-50-600. Ahmed et al. [30] investigated the roles of physical and chemical characteristics of activated carbon for the NH_3-SCR reaction and reported that chemical properties of activated carbons such as surface oxide and mineral matter were more important factors for de-NO_x performance than the physical properties, including specific surface area and pore structure. Therefore, it is contended that the functional groups that developed on the surface of SCW-50-700 and SCW-50-800 functioned as active sites on which NH_3 can be adsorbed, leading to a higher NO_x removal efficiency than SCW-50-600.

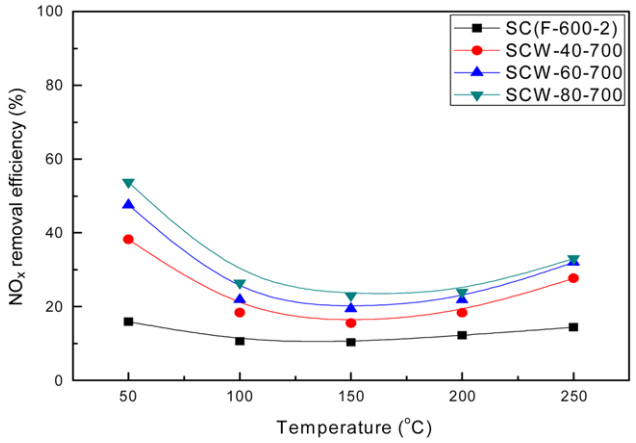

Fig. 10. Effect of moisture concentration on NO_x removal efficiency at different de-NO_x process temperatures.

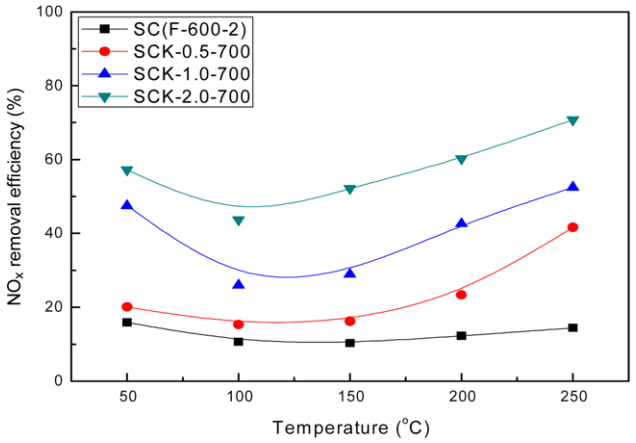

Fig. 12. Effect of KOH/char ratio on NO_x removal efficiency at different de-NO_x process temperatures.

Fig. 10 shows the de-NO_x performance of the SCWs activated at different water vapor concentrations. The NO_x removal efficiency increased as the water vapor concentration increased from 40 to 80 vol% throughout the temperature range tested. The FT-IR (Fig. 2) and NH_3-TPD (Table 4) analyses results suggest that increased water vapor concentration promotes oxygen function group development on the char surface, thus creating more active sites that enhance de-NO_x performance.

As shown in Fig. 9 and Fig. 10, NO_x removal efficiency was highest at 50 °C and showed minimum value around 150 °C. At an even higher temperature of 150 °C, however, the NO_x removal efficiency increased again, making the efficiency curve V shaped. For carbon-based catalysts, such removal efficiencies were the general trend. It is reported that in the presence of carbon catalysts, two different mechanisms may be operative in this process: adsorption of NO_x at low temperature (T<150 °C), and reaction at higher temperature (T>150 °C) [35].

2-2. SCKs

Fig. 11 shows the de-NO_x performances of SCKs activated at different temperatures as a function of the de-NO_x process temperature. Throughout the temperature range tested (50-250 °C), the NO_x removal efficiency decreased as the activation temperature increased. The NO_x removal efficiencies of SCK-1.0-700 and SCK-1.0-800 were shown to be lower than that of SCK-1.0-600, although the specific surface area and total pore volume of SCK-1.0-700 and SCK-1.0-800 were measured to be larger than those of SCK-1.0-600 (Table 3). As discussed earlier, this result can be attributed to the destruction of oxygen functional groups at high temperatures, leading to decreased NH_3 adsorption (Table 4) and de-NO_x performance.

Fig. 12 shows the NO_x removal efficiencies of SCKs activated with different KOH/char ratios. Throughout the temperature range tested (50-250 °C), the de-NO_x efficiency increased with KOH/char ratio. It is believed that development of more oxygen functional groups at a higher KOH/char ratio (Fig. 8) resulted in increased NH_3 adsorption (Table 4) and, in turn, increased NO_x removal due to reaction between adsorbed NH_3 and NO.

Fig. 13 compares the NO_x removal efficiencies of SCK-1.0-700, SCK-2.0-700 and SCK-2.0-600 with that of commercial activated carbon. The commercial activated carbon showed higher NO_x removal efficiencies than SCK-1.0-700 at 50 °C and 100 °C, whereas

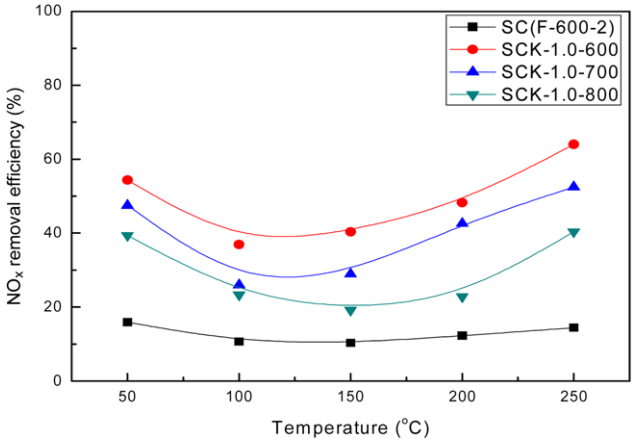

Fig. 11. Effect of activation temperature on NO_x removal efficiency of SCKs at different de-NO_x process temperatures.

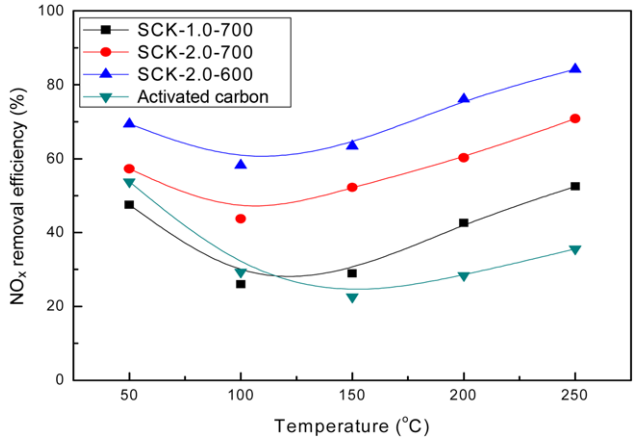

Fig. 13. NO_x removal efficiency comparison between two SCKs and a commercial activated carbon at different de-NO_x process temperatures.

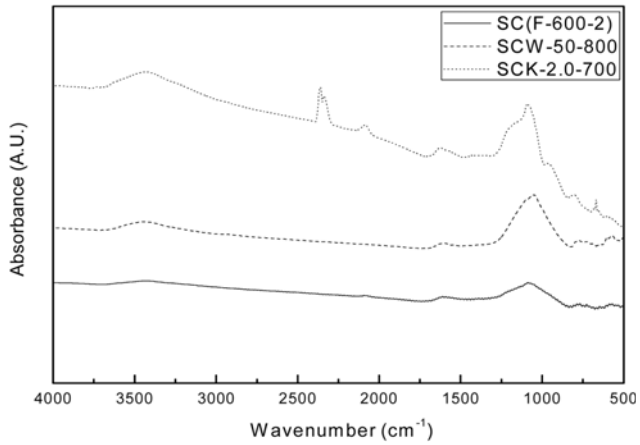

Fig. 14. Comparison of FT-IR spectra of SCK, SCW and SC.

the de-NO_x capability of the commercial activated carbon was lower above 150 °C. The SCK-2.0-700 and SCK-2.0-600 demonstrated higher NO_x removal efficiencies than the commercial activated carbon at all temperatures.

As shown in Fig. 11 and Fig. 12, NO_x removal efficiency was high at 50 °C and showed minimum value around 100-150 °C. At an even higher temperature of 150 °C, however, the NO_x removal efficiency increased again, making the efficiency curve V shaped. As discussed in 2.1, for carbon-based catalysts, such removal efficiencies were the general trend. It is reported that in the presence of carbon catalysts, two different mechanisms may be operative in this process: adsorption of NO_x at low temperature (T<150 °C), and reaction at higher temperature (T>150 °C) [35].

In general, activated sludges such as SCW and SCK showed higher catalytic NO_x removal efficiency than sludge char (SC-F-600-2) as shown in Figs. 9-12. Furthermore, SCK carbons showed higher catalytic NO_x removal efficiency than SCW carbons due to their higher surface area, oxygen functional group (Fig. 14) and increased NH_3 adsorption. Meanwhile, some SCW carbons such as SCW-50-800 showed similar NO_x removal activities with some SCK carbons such as SCK-0.5-700. SCW carbons contained almost metal components such as Fe and Ca while for SCK carbons, significant amounts of metals were washed out by HCl treatment (e.g, Ca was removed above 90 wt% by HCl treatment). Therefore, similar activities of some SCW and SCK carbons might be ascribed to the presence of metal components. However, further investigation is required on the exact role of metal components such as Ca and Fe in sludge char for NO_x removal.

CONCLUSIONS

The de-NO_x performance of carbon catalysts produced by activating sewage sludge char was evaluated. The char was activated either physically with water vapor or chemically with KOH. The effects of activation temperature and activation agent amount on the NO_x removal efficiency of the activated chars were investigated. The specific surface area and pore volume of the SCW, physically activated sludge char, increased with activation temperature. The specific surface area was largest when the water vapor content was 60 vol%, whereas the pore volume was largest when the water vapor content was 80 vol%. It was observed that the specific surface area and pore volume did not increase through physical activation to the extent that other studies report in the literature. The speculated cause is that high ash content in the sewage sludge inhibits pore generation during physical activation. As for SCK, chemically activated sludge char, the specific surface area and pore volume increased with KOH/char ratio and with activation temperature. Compared to physical activation, the change in the surface and pore structure by chemical activation was remarkable, suggesting that chemical activation is an appropriate method for producing activated char with a large specific surface area and pore volume from sewage sludge. The de-NO_x performance of activated chars is influenced more by chemical properties (oxygen functional groups, active sites) than by physical properties (specific surface area, pore volume). The SCK-2.0-700 and SCK-2.0-600, which demonstrated higher de-NO_x performance than commercial activated carbon throughout the entire temperature range tested in this study, may be one of the candidates for commercial activated carbons in SCR processes.

REFERENCES

1. S. Sun, J. Zhang, X. Hu, P. Qiu, J. Qian and Y. Qin, *Korean J. Chem. Eng.*, **26**, 554 (2009).
2. M. Y. Kim, K. W. Lee, J. H. Park, C. H. Shin, J. Lee and G. Seo, *Korean J. Chem. Eng.*, **27**, 76 (2010).
3. C. Ryu, K. Shim and S. Choi, *KSME J. B*, **23**, 548 (1999).
4. T. D. B. Nguyen, T. H. Kang, Y. I. Lim, W. H. Eom, S. J. Kim and K. S. Yoo, *Chem. Eng. J.*, **152**, 36 (2009).
5. J. C. Choi, C. H. Cho, K. E. Jeong, J. K. Jeon, J. H. Yim and Y. K. Park, *J. Korean Ind. Eng. Chem.*, **19**, 92 (2008).
6. F. Nakajima and I. Hamada, *Catal. Today*, **29**, 109 (1996).
7. M. Kang, E. D. Park, J. M. Kim and J. E. Yie, *Korean J. Chem. Eng.*, **26**, 86 (2009).
8. J. H. Choi, J. H. Kim, Y. C. Bak, R. Amal and J. Scott, *Korean J. Chem. Eng.*, **22**, 844 (2005).
9. A. Boyano, M. E. Galvez, R. Moliner and M. J. Lazaro, *Catal. Today*, **137**, 209 (2008).
10. J. Muñiz, G. Marbán and A. B. Fuertes, *Appl. Catal. B: Environ.*, **27**, 27 (2000).
11. H. Teng, Y. J. Chang and C. T. Hsieh, *Carbon*, **39**, 1981 (2001).
12. H. Jüntgen, *Erdöl und Kolhe*, **39**, 546 (1986).
13. G. S. Szyma´nski, T. Grzybek and H. Papp, *Catal. Today*, **90**, 51 (2004).
14. G. Marbán, R. Antuña and A. B. Fuertes, *Appl. Catal. B: Environ.*, **41**, 323 (2003).
15. J. Laine, A. Calafat and M. Labady, *Carbon*, **27**, 191 (1989).
16. J. Laine and A. Calafat, *Carbon*, **29**, 949 (1991).
17. B. S. Girgis and A. N. A. El-Hendawy, *Micropor. Mesopor. Mater.*, **52**, 105 (2002).
18. J. S. Cha, J. C. Choi, J. H. Ko, Y. K. Park, S. H. Park, K. E. Jeong, S. S. Kim and J. K. Jeon, *Chem. Eng. J.*, **156**, 321 (2010).
19. Z. Zhao, W. Li and B. Li, *Fuel*, **81**, 1559 (2002).
20. M. O. Marin, C. F. Gonzalez, A. M. Garcia and V. Gomezserrano, *Appl. Sur. Sci.*, **252**, 5967 (2006).
21. A. C. Lua and T. Yang, *J. Coll. Interf. Sci.*, **274**, 594 (2004).
22. T. Yang and A. C. Lua, *J. Coll. Interf. Sci.*, **267**, 408 (2003).
23. M. F. Tennant and D. W. Mazyck, *Carbon*, **41**, 2195 (2003).

24. R. C. Giberson and J. P. Walker, *Carbon*, **3**, 521 (1966).
25. P. L. Walker Jr., *Carbon*, **34**, 1297 (1996).
26. M. J. Lázaro, M. E. Gálvez, S. Artal, J. M. Palacios and R. Moliner, *J. Anal. Appl. Pyrolysis*, **78**, 301 (2007).
27. C. Bouchelta, M. S. Medjram, O. Bertrand and J. P. Bellat, *J. Anal. Appl. Pyrolysis*, **82**, 70 (2008).
28. F. C. Wu, R. L. Tseng and C. C. Hu, *Micropo. Mesopo. Mater.*, **80**, 95 (2005).
29. G. López, M. Olazar, M. Artetxe, M. Amutio, G. Elordi and J. Bilbao, *J. Anal. Appl. Pyrolysis*, **85**, 539 (2009).
30. S. N. Ahmed, J. M. Stencel, F. J. Derbyshire and R. M. Baldwin, *Fuel Process.Technol.*, **34**, 123 (1993).
31. J. Laine and A. Calafat, *Carbon*, **29**, 949 (1991).
32. F. C. Wu, R. L. Tseng and C. C. Hu, *Micropor. Mesopor. Mater.*, **80**, 95 (2005).
33. A. Ahmadpour and D. D. Do, *Carbon*, **35**, 1723 (1997).
34. F. Caturla, M. M. Sabio and F. R. Reinoso, *Carbon*, **29**, 999 (1991).
35. J. L. Figueiredo and M. F. R. Pereira, in *Carbon Materials for Catalysis*, P. Serp and J. L. Figueiredo Eds., John Wiley & Sons, Inc., Hoboken, New Jersey (2009).